ELSEVIER

Physica A 303 (2002) 410–420

PHYSICA A

www.elsevier.com/locate/physa

Short-term memories in lattices of inductively coupled AC-driven circuits

Antônio M. Batista[1], Ricardo L. Viana*

Departamento de Física, Universidade Federal do Paraná, C.P. 19081, 81531-990 Curitiba, PR, Brazil

Received 12 June 2001; received in revised form 14 September 2001

Abstract

Short-term memory formation is a collective effect displayed by driven spatiotemporal dynamical systems, in which the injected signal is echoed back in many different ways due to the coupling effect. The existence of multiple short-term memories enables us to use these systems to encode signals. We present numerical evidence of short-term memory generation in a lattice of AC-driven circuits with inductive coupling. The multiple configurations exhibited by this oscillator chain can be used to encode graphical characters.

PACS: 05.45.Xt; 05.45.Ra

Keywords: Short-term memories; Coupled circuits; Coupled oscillator chains

1. Introduction

The most common context in which a physicist works with concepts of memory storage and retrieval is a neural network. For example, in a network of binary neurons with a specified connectivity prescription, there are some configurations of the system that minimize some Ising energy, and these are usually related with patterns memorized by the network [1,2]. Such patterns may persist for an indefinite time unless some kind of external perturbation or noise alters the situation. The connection between memorized patterns in neural networks and learning processes is a subject of great interest and vigorous research [3,4].

* Corresponding author.
E-mail address: viana@fisica.ufpr.br (R.L. Viana).
[1] Permanent address: Departamento de Matemática e Estatística, Universidade Estadual de Ponta Grossa, 84030-000 Ponta Grossa, PR, Brazil.

0378-4371/02/$ - see front matter
PII: S0378-4371(01)00503-9

Besides these permanent or long-term memories, a different kind of memory has been also observed in the form of a collective effect displayed by lattices of coupled dynamical systems with external driving. Due to the spatial extension of the system provided by the lattice structure, the external driving may be echoed on as long as the forcing is sustained. This effect has been called a *short-term memory* and it was first described by Coppersmith et al. [5] to interpret results of a charge density wave experiment in $NbSe_3$, in which the memory encoding manifest as a synchronization of the crystal responses to a periodic train of driving electric pulses. A coupled map lattice (CML) with external periodic input was proposed to explain the existence of short-time memory formation in this experiment [5].

The use of a coupled map lattice [6,7], in which space and time are discrete but with a continuous state variable attached to each lattice site, may be advantageous from the point of view of a neural network, when compared with usual Ising-type models as the Hopfield model [8]. As the state variable can assume any real value within a given range, a convenient partitioning of this domain enables us to encode complex information. This is important in terms of the memory storage capacity of the lattice since we could design, at least in principle, smaller networks with coupled map lattices, while retaining the overall memory capacity.

A step forward in this direction was the observation that a coupled map lattice may store multiple short-term memories. This was verified by using a weakly nonlinear map for the local dynamics at each site [9], but it was suggested that the addition of small external noise to a linear map could provide the same effect [5]. In Ref. [9], we applied the formation of multiple short-term memories to encode symbols in a pixel matrix. A rule for storing a given sequence of pixels was translated into analytical expressions for some control parameters, like the input amplitudes or coupling strengths. The existence of both short- and long-time memories in a coupled map lattice (using a bit-string formulation in a shape space) has been recently proposed to study immune response to antigen presentation. In this case, the memory effects are related to the mechanism of vaccination [10].

In this paper, we consider a dynamical system of physical relevance consisting of a lattice of inductively coupled AC-driven circuits, which exhibits multiple short-term memories echoing back the periodic signals injected to the lattice units. The coupled system of differential equations for the circuits is numerically solved, and we define a suitable quantity (curvature variable) to characterize the memorized spatiotemporal patterns. These patterns, after a convenient partitioning of the curvature variable domain, are used to encode information. As an illustrative example we chose the Braille language system.

Previous studies have characterized other types of spatiotemporal patterns in lattices of coupled electrical circuits [11]. The dynamical system we study is a lattice of coupled continuous-time oscillators, but we show that the same relevant effects are displayed when a coupled map lattice is written as a discretized version of the system. The obtaining of this coupled map lattice enables us to obtain a control law for information coding, as has been done in Ref. [9] for a simpler system.

This paper is organized as follows: Section 2 introduces the chain of inductively coupled circuits with periodic forcing. In Section 3 we define short-time memories in such systems and derive a corresponding coupled map lattice. Section 4 is devoted to a numerical analysis of the effect of parameter noise in the short-time memory storage. The last section contains our conclusions.

2. Coupled circuit lattice

The coupled circuit lattice is depicted in Fig. 1. Let $i^{(k)}(t)$ be the current intensity in the single mesh of the kth circuit at time t, containing two equal self-inductances $L^{(k)}$ and resistances $R^{(k)}$, driven by AC-sources $V^{(k)}(t)=V_0^{(k)}\sin(\omega t)$. Each circuit but the two boundaries is inductively coupled to its nearest neighbors with mutual inductances $M^{(k)}$. On the other hand, we neglect the mutual inductance between the inductors present in a same circuit.

The mesh equation for the current in the kth circuit is written down as

$$2L^{(k)}\frac{\mathrm{d}i^{(k)}(t)}{\mathrm{d}t}+R^{(k)}i^{(k)}(t)=M^{(k)}\left[\frac{\mathrm{d}i^{(k-1)}(t)}{\mathrm{d}t}+\frac{\mathrm{d}i^{(k+1)}(t)}{\mathrm{d}t}\right]+V^{(k)}(t) \tag{1}$$

with $k=1,2,\ldots,N$. The strength of the inductive coupling between two adjacent circuits is given by [12]

$$\varepsilon^{(k)}=\frac{M^{(k)}}{\sqrt{L^{(k)}L^{(k+1)}}}\,. \tag{2}$$

We will consider the case in which $L^{(1)}=L^{(2)}=\cdots=L$, $R^{(1)}=R^{(2)}=\cdots=R$, and $M^{(1)}=M^{(2)}=\cdots=M$, so that $M=\varepsilon L$, with $|\varepsilon|\leqslant 1$.

It is convenient to use non-dimensional quantities so that we define a normalized current $i'^{(k)}=i^{(k)}/\mathscr{I}$, where $\mathscr{I}$ is a characteristic value, and $t'=t/\tau$, where τ is an inductive time constant for each circuit. In this way, the lattice system is rewritten as

$$\frac{\mathrm{d}i'^{(k)}(t')}{\mathrm{d}t'}-\frac{\varepsilon}{2}\left[\frac{\mathrm{d}i'^{(k-1)}(t')}{\mathrm{d}t'}+\frac{\mathrm{d}i'^{(k+1)}(t')}{\mathrm{d}t'}\right]=-ai'^{(k)}+b^{(k)}\,, \tag{3}$$

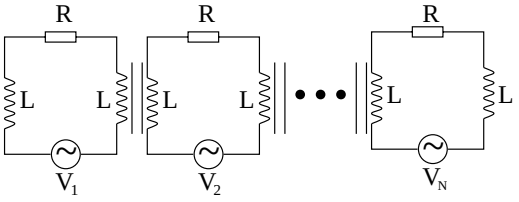

Fig. 1. Lattice of inductively coupled AC-driven circuits.

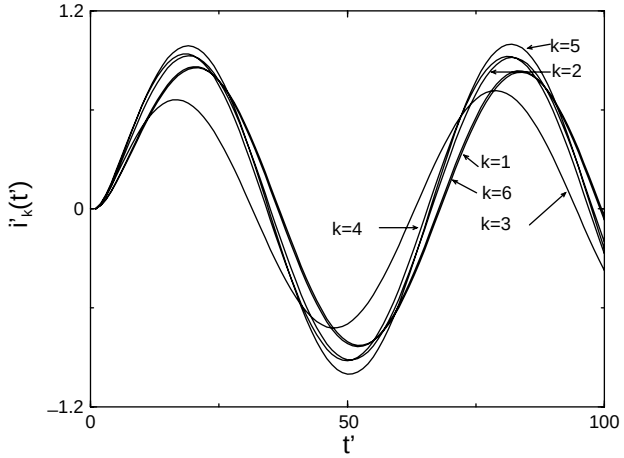

Fig. 2. Time series of the currents for each circuit in a lattice with $N=6$, $\varepsilon=0.83$, $a=0.1$, $\omega=0.1$, $B^{(i)}=0.1$ for $i\neq 3$, and $B^{(3)}=0.05$.

where we define

$$a=\frac{R\tau}{2L}\,, \tag{4}$$

$$b^{(k)}(t')=\frac{\tau}{2L\mathscr{I}}V^{(k)}(t')\equiv B^{(k)}\sin(\omega' t')\,. \tag{5}$$

From now on we drop the primes from the variables for ease of notation.

System (3) is not directly solvable by using common differential equation integrators like Runge–Kutta-type schemes, since there are three first-order derivatives in each coupled equation. We have to solve first a linear algebraic system, where the square matrix of coefficients is tridiagonal and thus may be factorized using LU decomposition [13]. This enables us to integrate (3), by using fixed boundary conditions: $i^{(0)}(t)=0$ and $i^{(N+1)}(t)=0$ for all times, and a uniform initial condition $i^{(k)}(0)=0$ for all sites. An example of solution for this system is shown in Fig. 2, where we plot time series of the currents for each circuit in a small lattice of $N=6$ elements. Note that all of them oscillate with small amplitude differences and certain mutual dephasage. Hence, they are not synchronized in phase and exhibit some frequency mismatch.

3. Short-time memories

The external periodic inputs applied to the spatiotemporal system described in the previous section are echoed by the circuit lattice due to the diffusion effect caused by oscillator coupling. The lattice response to these inputs is manifested in the form of short-time memories. These short-term memories are best revealed by means of a curvature variable, defined for each circuit as the amplitude of the current, after its value

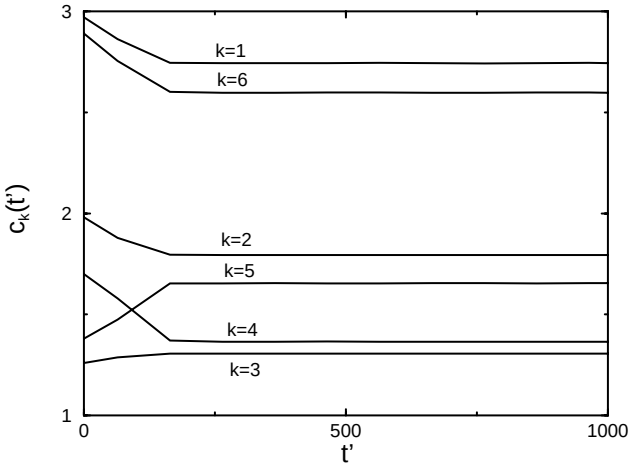

Fig. 3. Curvature variables versus time in a lattice with $N=6$, $\varepsilon=0.83$, $a=0.1$, $\omega=0.1$, $B^{(i)}=0.6$ for $i\neq 3$, and $B^{(3)}=0.3$.

is updated due to coupling

$$c^{(k)}(t)=\max\left|i^{(k)}(t)-\frac{\varepsilon}{2}(i^{(k-1)}(t)+i^{(k+1)}(t))\right|\,, \tag{6}$$

where we take the maximum value of the argument with respect to one complete cycle or period $T=2\pi/\omega$ of the external forcing. Hence, $c^{(k)}(t)$ are consecutive local maxima, in the same way we sample phase-space variables in a stroboscopic (time—T) map for a periodically forced dynamical system [14].

We assign a constant value for $c^{(k)}$ to a given memory, and it is of a short-term nature because if the external input vanishes so do the memories themselves. After a usually short transient, the curvature variables settle down at multiple stationary values, as shown in Fig. 3 for a lattice with $N=6$ circuits. In this example the circuit with $k=3$ has an input amplitude of $B^{(3)}=0.3$, whereas the remaining elements have $B^{(k\neq 3)}=0.6$. The corresponding values of the curvature variables depend on the external input amplitudes. To illustrate this fact, in Fig. 4 we vary the amplitude on the $k=3$ site, keeping all other circuits unchanged, and follow the resulting stationary values of $c^{(k)}$. This suggests that we may use $B^{(3)}$ (or any other isolated input amplitude) as a kind of control parameter so that we can obtain different memorized patterns just by varying this external parameter.

The fact that multiple memories are formed (a different value of $c^{(k)}$ for each coupled circuit) allows us to encode information by partitioning adequately the curvature variable domain. A lattice with $N=6$ elements is sufficient to encode symbols in a 3×2 pixel matrix, as those used in the Braille language system [see Fig. 5(a)]. The Braille system uses groups of points to represent graphic symbols. Each Braille cell consists of six points (two columns and three rows) and may store 63 different symbols

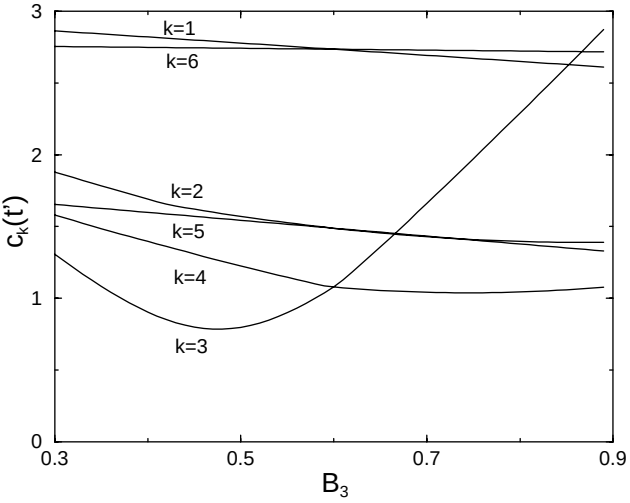

Fig. 4. Curvature variables versus input amplitude $B^{(3)}$ for the same parameters as in Fig. 3.

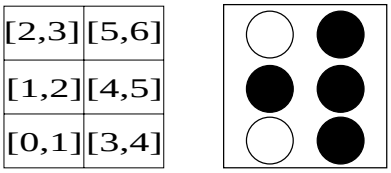

Fig. 5. (a) Pixel matrix and partitions of the domain of the curvature variables; (b) Braille symbol corresponding to the letter "W".

that are perceived by tactical sensitivity.[2] We assign to each pixel in Fig. 5(a) a given sub-interval of the curvature variable domain $c^{(k)} \in [0,6]$. When, for a given circuit, the curvature presents a value belonging to any of these sub-intervals, the corresponding matrix pixel is filled in. A pattern is formed by superposing six of such matrices, and it is related to the symbols belonging to the Braille language. Obviously, there are many (in fact, infinite) different choices of the curvature values leading to the same symbols.

A systematic way to encode information in such a lattice would be to obtain an analytic rule whereby we compute the necessary values of the curvature variable that yield a given symbolic sequence. Whereas this is not feasible by using the original system of coupled differential equations (3), it is rather easy to implement in coupled map lattices. Such approach has been used in Ref. [9] for encoding information in a lattice of weakly nonlinear maps with external driving. In our system, this reduction

[2] A comprehensive source of information about the Braille system can be found at the American Council of the Blind website: http://www.acb.org/Resources/braille.html.

involves a discretization of the time derivatives, where $i^{(k)}(t)$ is replaced by its value at discrete time $n=0,1,2,\ldots$, which we denote $i_n^{(k)}$.

A coupled map lattice with periodic forcing for the oscillator chain (3) is

$$i_{n+1}^{(k)} - \frac{\varepsilon}{2}\left(i_{n+1}^{(k-1)} + i_{n+1}^{(k+1)}\right) = (1-a)\, i_n^{(k)} + b_n^{(k)} - \frac{\varepsilon}{2}\left(i_n^{(k-1)} + i_n^{(k+1)}\right) , \tag{7}$$

where $b_n^{(k)} = B^{(k)} \sin(\omega n)$. It should be remarked here that this discretization is valid provided we have a period for the external input much greater than the discretization period $\Delta t = 1$; i.e., it is necessary that $\omega \ll 1$ for (7) being an acceptable discretized form of (3). The CML (7) is not written in a usual way, though, since there are three unknown variables at advanced time $n+1$. This makes a system of coupled algebraic equations that has to be solved before advancing to further time steps, but the necessary matrix manipulations are essentially the same as in the continuous time case. We have verified that the CML (7) gives results in excellent agreement with those obtained by using a chain of coupled circuits.

In the time-discretized system the curvature variables are redefined as

$$C_n^{(k)} = \max \left| i_n^{(k)} - \frac{\varepsilon}{2}\left(i_n^{(k-1)} + i_n^{(k+1)}\right) \right| , \tag{8}$$

where the maximum value is computed for a complete cycle of external forcing, as in Eq. (6). A memorized pattern is considered to be a set of stationary values of the curvature variables. However, the use of a CML is advantageous when compared with the continuous oscillator chain, since a CML enables us to write an explicit rule that gives the necessary value of the external input amplitudes $B_n^{(k)}$ for obtaining a given stationary target curvature $C^{(k)} = \mathscr{A}^{(k)}$. It turns out that this rule is

$$B_n^{(k)} = \frac{1}{\sin(\omega n)} \left\{ \mathscr{A}^{(k)} \sin[\omega(n+1)] + (a-1) i_n^{(k)} + \frac{\varepsilon}{2}\left(i_n^{(k-1)} + i_n^{(k+1)}\right) \right\} , \tag{9}$$

which can be used provided $\omega n \neq 2m\pi$ with $m = 0,1,2,\ldots$. If this occurs, however, we can easily circumvent the problem by adjusting the target curvature so as to give a finite value of $B^{(k)}$, without changing the pattern to be encoded.

As an example, let us encode the Braille symbol corresponding to the letter "W" [see Fig. 5(b)]. In order to fill in the matrix pixels yielding this symbol, we use a lattice with six sites and choose the following target curvature amplitudes (which are not the unique choice): $\mathscr{A}^{(1)} = 1$, $\mathscr{A}^{(2)} = 3$, $\mathscr{A}^{(3)} = 4$, $\mathscr{A}^{(4)} = 5$, and $\mathscr{A}^{(5)} = \mathscr{A}^{(6)} = 6$, the remaining parameters being the same as in Fig. 3. Putting these target values into Eq. (9) results in a sequence of values for $B_n^{(i)}$ which typically varies with time.

For the example here considered we depict in Fig. 6 the values of one of such amplitudes, say $B_n^{(3)}$, as a function of time, showing that in most of the time only small inputs are necessary, with exception of large spikes which occur at regular time intervals. The corresponding time series for other lattice sites have qualitatively similar features, the difference being the height of the spikes. Remember that, for the sake of symbol encoding, it is sufficient to apply these variable external perturbations on a single circuit. The remaining coupled circuits continue to have sinusoidal external inputs with a constant amplitude.

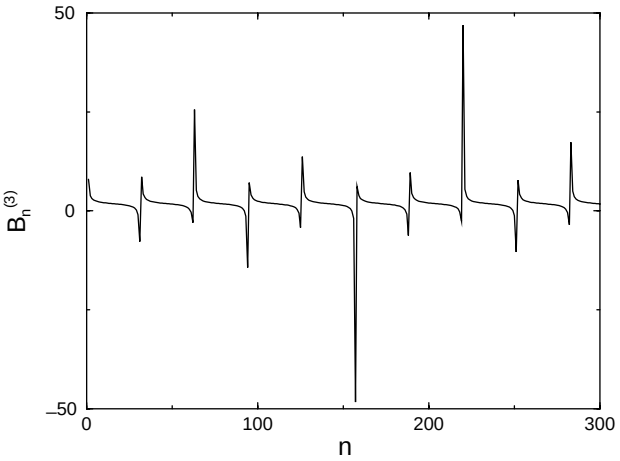

Fig. 6. Time series of the values of the input amplitude $B_n^{(3)}$ necessary to yield the Braille symbol corresponding to letter "W" in a coupled map lattice with $N = 6$ sites, and parameters $\varepsilon = 0.83$, $a = 0.1$, $\omega = 0.1$.

We remark that Fig. 6 does not present stationary values for $B_n^{(3)}$. In fact, this is the price we pay for using a control law, Eq. (9), that has an explicit dependence on time. This dependence comes from the oscillatory nature of the forcing in each circuit. If this forcing were a constant input, as in Ref. [9], a control law similar to (9) would be derived without explicit dependence in time, so we would have stationary and constant values for $B^{(3)}$.

4. The effect of noise

The effect of extrinsic noise cannot be overlooked when one has in mind a laboratory implementation of coupled electric oscillators. In particular, additive noise may come from uncertainties in the values of the parameters characterizing each circuit, as its resistances, inductances and external e.m.f. Thus, we should assess the effect of noise on the memory storage capacity of our system, inserting noise in one of the circuit parameters, as for example

$$a_n^{(k)} = a \pm \delta_1 r_{n,k} \,, \tag{10}$$

where a is the nominal value of the parameter given by Eq. (4), $\delta_1 > 0$ is a noise level, and $r_{n,k}$ are random variables with zero mean and uniform distribution in the interval $[0, 1]$. In Fig. 7, we plot the stationary values of the curvature variables shown in Fig. 3, versus the noise level δ_1 in the parameter a. We see that as the noise level builds up, the stationary values of the curvatures are no longer constants but become distributed over bounded tongue-like intervals with increasing width, represented as blurred regions in Fig. 7.

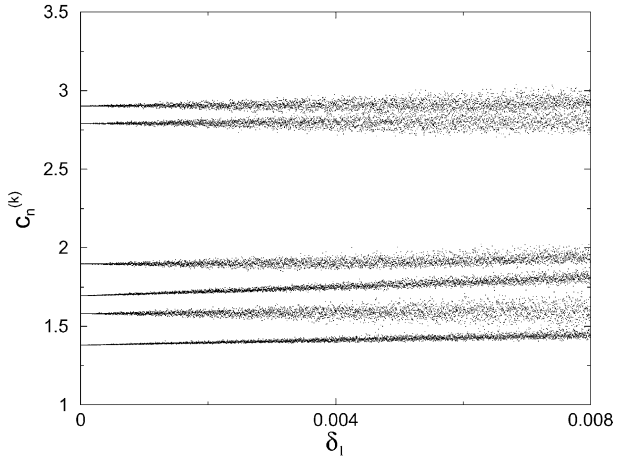

Fig. 7. Stationary values of the curvature variables versus the noise level in the circuit parameter a. The remaining parameters are the same as in Fig. 3.

A possible source of trouble is when the blurred tongues intercept the partition boundaries of the curvature interval $[0,6]$. However, this difficulty could in principle be circumvented by modifying the partition boundaries either by moving them or by making a non-uniform boundary distribution. A more difficult problem, however, is when two blurred regions overlap, so that the corresponding curvature variables become indistinguishable. In the case of Fig. 7 this begins to occur for noise levels above 0.4%, which may be considered as the limit of application of our encoding scheme, at least for this particular curvature partition. In general, for high noise levels virtually any partition is likely to present some overlap, and new coding schemes would be necessary.

We also have included noise in the external input amplitudes

$$B_n^{(k)} = B^{(k)} \pm \delta_2 r_{n,k} \,, \tag{11}$$

where $B^{(k)}$ are the specified input amplitudes used in Fig. 3, and δ_2 is another noise level. A question very similar to that posed by the overlap of blurred curvature amplitudes, is to what extent we may increase both noise levels and still have reliable results. A detailed analysis of this question would be rather involved since the intervals for amplitude overlap vary with many parameters, including the curvature values themselves.

A simpler way to give some insight on this effect is to consider for which pairs of noise levels (δ_1, δ_2) we have a difference between the noisy and the noiseless curvature values higher than a given tolerance, say 1.0%. In Fig. 8, we use black dots to plot, in the parameter plane, the values of δ_1 and δ_2 for which $|C^{(k)} - C^{(k)}(\delta_1 = \delta_2 = 0)| \geqslant 0.01$, for a given site k (stationary values are taken). This gives a rough idea of what noise levels may affect the encoding scheme up to a given tolerance. The distribution of the black dots shows a clear increase for higher noise, and it is not symmetric—we allow noise levels in the b-variable to be almost one order of magnitude higher than

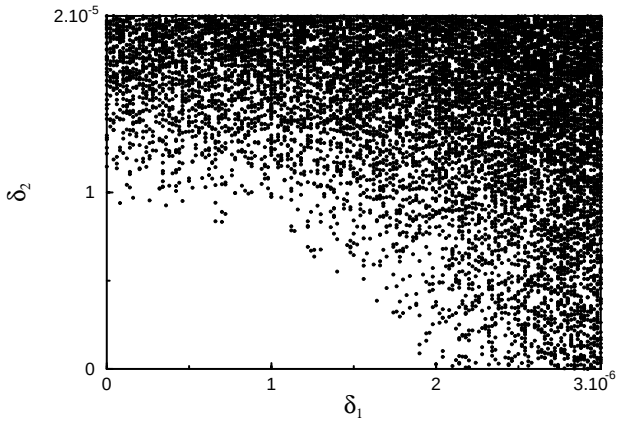

Fig. 8. Black dots indicate noise level pairs (in the circuit parameters and input amplitudes) which affect any noiseless curvature variable from one part in a hundred or more.

the corresponding noise levels in the *a*-variable. Hence, the coupled lattice seems to be more robust to noise present in the external inputs than in its parameters.

5. Conclusions

We have extended the concept of short-time memory formation in spatially extended systems, introduced by Coppersmith et al. [5], to a chain of inductively coupled AC-driven circuits. These memories show up as stationary values of suitably defined curvature variables. Since multiple memories can be generated, we have numerically shown a possible way to encode symbolic sequences by using a pixel matrix, where to each pixel we assign a given circuit. Discretizing the system of equations, we have obtained a coupled map lattice so that we can write an explicit rule for the values of the perturbing input amplitudes which are necessary to yield a desired symbolic sequence. We have chosen as an illustrative example, some symbolic sequences of the Braille language; but with larger lattices other and more complex sequences can be stored. The effects of noise on the circuit parameters and input amplitudes were considered, and we have shown that the encoding scheme is reasonably robust to noise, even though some modification in the partitions may be required.

Acknowledgements

This work was made possible by partial financial support from CNPq (Conselho Nacional de Desenvolvimento Científico e Tecnológico), Fundação Araucária (State of Paraná, Brazil), and FUNPAR (UFPR).

References

[1] J.J. Hopfield, Proc. Natl. Acad. Sci. USA 79 (1982) 2254.
[2] J.J. Hopfield, D.W. Tank, Science 233 (1986) 625.
[3] H. Gutfreund, Physica A 163 (1990) 373.
[4] A. Engel, C. Van Den Broeck, Statistical Mechanics of Learning, Cambridge University Press, Cambridge, 2001.
[5] S.N. Coppersmith, T.C. Jones, L.P. Kadanoff, A. Levine, J.P. McCarten, S.R. Nagel, S.C. Venkataramani, X. Wu, Phys. Rev. Lett. 78 (1997) 3983.
[6] J.P. Crutchfield, K. Kaneko, Phenomenology of spatio-temporal chaos, in: Hao Bai-Lin (Ed.), Directions in Chaos, Vol. 1, World Scientific, Singapore, 1987.
[7] K. Kaneko, The coupled map lattice, in: K. Kaneko (Ed.), Theory and Applications of Coupled Map Lattices, Wiley, Chichester, 1993.
[8] H. Nozawa, Chaos 2 (1992) 377.
[9] A.M. Batista, R.L. Viana, S.R. Lopes, Phys. Rev. E 61 (2000) 5990.
[10] R.M.C. de Almeida, M.C.B. Lagreca, K. Aquere Filho, R.L. Viana, Short and long time memory storage in a coupled map lattice model of immune response, 2001, preprint.
[11] A.P. Munuzuri, V. Perezmunuzuri, M. Gomezgesteira, L.O. Chua, V. Perezvillar, Int. J. Biff. Chaos 5 (1995) 17.
[12] J.R. Reitz, F.J. Milford, R.W. Christy, Foundations of Electromagnetic Theory, Addison-Wesley, Reading, MA, 1980.
[13] W.H. Press, S.A. Teukolsky, W.T. Vetterling, B.P. Flannery, Numerical Recipes in C, Cambridge University Press, Cambridge, 1995.
[14] E. Ott, Chaos in Dynamical Systems, Cambridge University Press, Cambridge, 1994.